MODELLING AND SIMULATION OF ECAP AND P-ECAP TECHNIQUES OF GRAIN INDUCEMENT IN MILD STEEL

D. E. Esezobor[1], *H. O. Onovo[1], A. O. Ojo[2], M. A. Bodude[1]
[1]Department of Metallurgical and Materials Engineering, University of Lagos, Nigeria.
[2]Department of Mechanical Engineering, University of Manitoba, Canada.
E-mail: desezobor@unilag.edu.ng[1], honovo@ unilag.edu.ng [1],
olanrewaju.Ojo@umanitoba.ca[2], mbodude@ unilag.edu.ng[1]
Corresponding Author: honovo@ unilag.edu.ng, +2348080831194

ABSTRACT
Due to major obstacles associated with the powder consolidation methods of producing bulk nano materials such as high cost, contamination and porosity, severe plastic deformation (SPD) technology, specifically the equal channels angular pressing (ECAP) technique is used with modifications to numerically simulate the much needed grain refinement in steel. Attempts are made in this study to investigate influence of processing parameters such as deformation routes, temperature, load and number of processing passes on the degree of strain inducement in steel. This study however, aimed at developing fourth generation metals of exceptional strength, formability and toughness. The materials used in this work include conventional mild steel and ABAQUS commercial software. Simulation and modeling of the proposed deformation and ECAP techniques were done using finite element based-method (FEM). The results obtained indicate that the desired performance index of the metal is dependent on the state of the metal prior to ECAP and the degree of deformation.

Keywords: deformation, formability, strain, strength, toughness

1. INTRODUCTION

Properties of engineering materials are of great importance in engineering practice. An engineering material cannot perform in practice beyond its capability, which is a function of its properties. A material may be preferred; owing to its superior property over its contemporary materials. Three basic properties of metals (strength, toughness and formability i.e. ultra-plasticity, ability of a material to be deformed plastically without deformation defect) are of great importance to many engineering applications particularly in automobiles. But in practice, these three fundamental properties have not been achieved in one metal, due to the technical disparity existing in metals with varied grains sizes.

Hall and Petch (1951), Segal et al. (1981), Valiev et al. (1991) and Iwahashi et al. (1998), proved the assertion that metal's strength/hardness have a direct

116

correlation with its grain size. Materials' properties such as the strength/or hardness of metals increases as the grain sizes decreases.

One of the major research-focused areas in materials engineering in recent times is the application of grain refinement of metals to achieve high strength, toughness and formability in a metal (Halfa, 2014). Interestingly, metals such as steel have gained wide industrial applications especially in automobile industries due to its high strength and high toughness, in other words reliability. The major issues associated with steel are weight related challenges such as green-house-gas (GHG) emission, lack of fuel economy, etc. This has led to decrease in the use of steel in automobiles, and its substitution is at the expense of high reliability.

However, the steel could be processed through grain refinement and in turn overcome the weight-strength issues that marred or decrease its usage in automobile. The feasibility lies for instance in a component where a 10mmthick steel with a specified strength would have been used to ensure a particular strength in service is available, approximately half the thickness of that steel with fine grains and accompanying greater strength could as well be used without compromising the strength, hence overall weight reduction is feasible with ultrafine grained steel (UFG).

Conventional methods of producing ultrafine grained steels includes: micro-alloying (Pickering, 1990 and Korczynsky, 1988), heat treatment (Sellars and Whiteman, 1979; Grange, 1966; and Wada and Eldis, 1982), advanced thermo mechanical processes (Zhao et al., 2011; Niikura et al., 2001; Najafi-Zadeh et al., 1992; and Ueji et al., 2002), large-strain warm deformation (Hanamura et al., 2004; and Sellars and Whiteman, 1979), rapid cooling and short interval multi-pass hot rolling (Toshiro et al., 2008), and powder consolidation (Halfa,2014). These techniques even though have been well developed are unsuccessful owing to technical challenges such as contamination, porosity, high cost, high pressure and lengthy heat treatment associated with them, and inability to develop bulk metals that are applicable to engineering structures. On the other hand, the SPD techniques (Valiev et al., 2003; Alexandrov and Valiev, 2001; and Stolyarov et al., 1999) have the capability of producing bulk nanostructured materials that are large enough for structural applications. Equal channel angular pressing (ECAP) is one of the outstanding SPD techniques that has been extensively studied. Its attractive procedure for many reasons, according to Segal et al. (2004) consists of its ability to be applied to fairly large billets and billets of different shapes and

cross-sections such as bars, rods, sheets, strips or flat plates (Segal et al., 2004; Bridgman, 1952; and Saunders and Nutting, 1984).

Since the introduction of ECAP process by Segal et al. (1981) the process has undergone so many modifications in the design of the die, the processing routes, and the use of other experimental and analytical parameters (Azushima et al., 2008; Langdon, 2011; Sanusi and Oliver, 2009; Alexander, 2007; Mishra et al., 2005; Rhodes et al., 1997; Mishra and Ma, 2005; Beygelzimer et al., 2004; Varyutkhin et al., 2006; Richert et al., 1999; and Valiev et al., 1991), in other to produce a material with superior properties through grain refinement. To convert a coarse-grained solid or bulk material into a material with nano-sized grains, it is technically necessary to impose an exceptionally high strain. This aids in introducing a high density of crystals dislocations, which subsequently re-arranged themselves to form an array of grain boundaries (Segal et al., 2004). From foregoing, conventional SPD process together with the modified techniques have been used by researchers to achieve grain size reduction from coarse to UFG level. The target however, is to obtain nano-scale grain-size, through appropriate modification that is received to attain novel nano level ($< 50nm$). This study is however apprehensive of the following difficulties such as limitations on the overall strains that may be imposed on the material via these procedures on one hand. Theses trains to be imposed on the materials using the technique may not be large enough to introduce nanostructures due to constraints associated with the overall workability of metallic alloys at cryogenic, ambient or relatively low temperatures (Segal et al., 2004).

According to Iwahashi et al. (1997), regardless of the attention given to the principles of ECAP (Segal et al., 2004) and its areas of applications (Iwahashi et al., 1997 and Segal et al., 1981), there exists the issue of estimating the magnitude of strain introduced into the samples using the ECAP technology. Some earlier assumptions concerning analytical estimation of strain were made in error and these were identified by Wang*et al*., (2013). Iwahashi et al., (1997) assuaged the incomplete information by deriving equations that could be used to estimate the magnitude of strain induced in a material, considering different die geometries, such as die (Φ) angles and angles of curvature (Ψ). They used the first principle to slot in Ψ in their analysis, which enabled them to derive a general equation solution for strain estimation.

Numerical simulation for the estimation of magnitude of strain inducement in metals offers more accurate information, as the amount of strain imposed per

discretized finite element could be obtained. The total and/or overall strain introduced into the metal can be evaluated. More also, the distribution of strain across the metal could also be presented with the aid of numerical spectrum.

Finite element method (FEM) simulations are helpful to estimate some correct parameters of ECAP device and pressing process such as geometrical parameters, the pressing speed of the ram, pressing temperature or load displacement curve (Sanusi and Oliver, 2009; and Valiev, 2003).The effects of pressing temperature on ultra-fine formation during hot ECAP is still a matter of intense debate. Consensus is however yet to be reached (Krishnaiahet al., 2004; and Sanusi and Oliver, 2009). The pressing temperature is a key factor in ECAP technique for determining and developing a material's microstructure. Yamashita et al. (2000) found that increasing the deformation temperature gives rise to increase in grain size with a corresponding decrease in the misorientation of strain-induced boundaries. Kommel et al. (2007) reported increase in ductility of UFG materials during low temperature annealing. Nevertheless, there is still dearth of information on the most appropriate ECAP processing temperature to date.

Table 1: SAE 1010 Compositional Analysis

Elements	Fe	C	Mn	P	S	Si
Content (%)	99.48	0.10	0.35	0.038	0.045	0.07

In this study, an attempt is made to establish, the appropriate processing temperature condition on the basis of the magnitude and distribution of imposed strain, a real-life simulations of plastic deformation through pre-deformation rolling of the specimen at room temperature to obtain a reasonable amount of strain in the material prior to entering the ECAP cavity with pre-determined die geometry. This novel method will offer many possible advantages, as most suitable approach to maximize volumetric strains inducement into the material. It is also possible to process different shapes of specimen, including bars, rods, sizeable sheets, strips, etc., via this method.

2.   METHODOLOGY

The material used in this study was SAE 1010steel which has percentage compositional analysis as contained in Table (1)with dimension of 200mm x 30mm.

In the modified ECAP setups, the material was deformed using cold rolling to approximately 6 percent reduction, prior to ECAP. The die angle was maintained

at angle 90° while the curvature angles were varied from 0° to 20° due to their proven capability of yielding maximum strain inducement. The setup with die angle 90° and curvature angle 20° was chosen as reference point.

The 2-dimensional schematic diagram of the model shown in Fig.(1) depicts the conceptual pre-deformation and ECAP technology.
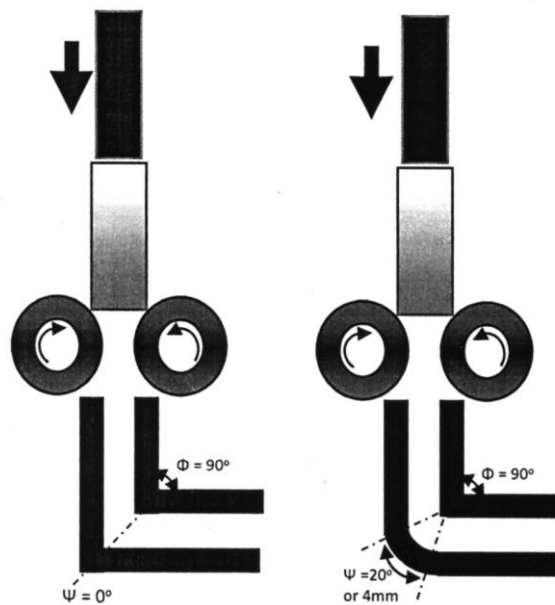

Figure 1: The conceptual pre-deformation and ECAP (P-ECAP) setup

The numerical modeling and simulation of the conventional rolling process, and ECAP setups with and without pre-deformation were conducted using the commercial ABAQUS software 6.13.1 version (SIMULIA, 2013). To obtain some useful simulation data, quasi-static tension experiments were carried-out at room temperature using MTS servo hydraulic machine which has an actuator of 11-kip rating. Calibrated load cell and extensometer attached to the MTS Servo hydraulic machine were used to measure the corresponding load and estimate the strain values.

The ECAP setup with pre-deformation was carried out at different pressing temperature conditions ($0.75T_m$, $0.5T_m$, $0.35T_m$, $0.3T_m$, $0.25T_m$, $0.15T_m$, $0.1T_m$, and room temperature, 25^oC), considering the basic elastic, plastic and thermal properties of steel.

120

Table 2: Material's Properties Considered During Simulation

Mechanical	Values	Thermo-Physical Properties	Values
Tensile strength, Ultimate (MPa)	390	Thermal expansion co-efficient (μm/m^{o}C)	12.2
Tensile Strength, Yield (MPa)	299	Thermal conductivity (W/m-K)	49.8
Elongation (%)	10	Specific heat Capacity (J/Kg-K)	460
Elastic modulus (GPa)	200	Melting Temp ^{o}C	1506
Poisson ratio	0.29	Density (Kg/m^3)	7700

III. RESULTS AND DISCUSSION

The results of the quasi-static tension test of SAE 1010 steel at room temperature, is shown in Fig. (2) as stress-strain curve as well as the evolved microstructure. Table (2) comprises some of the materials mechanical properties obtained from quasi-static tension test, as well as the physical properties used for simulation.
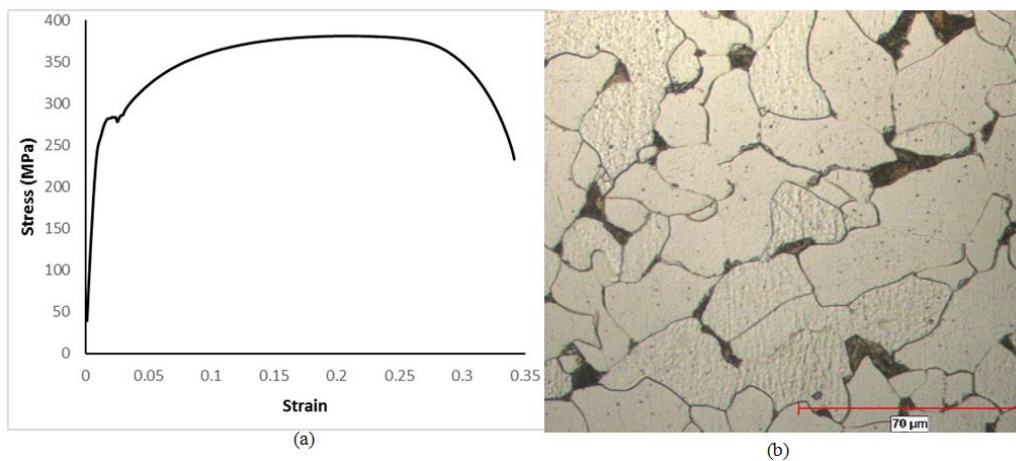
Figure 2:   Elastic – Plastic behavior of SAE 1030 Steel used at room temperature. Stress – Strain curve (a), and Optical micrograph at 100X magnification

The results of the plastic equivalent strain (PEEQ) inducement activities of mild steel at low and elevated temperatures is presented in Fig.(3). The low temperature shows a consistent higher values of strain across the discretized finite element number up to one thousand one hundred (1,100). The trend of strain inducement activities with this low temperature maintained a sinusoidal pathway, throughout the heated domain.
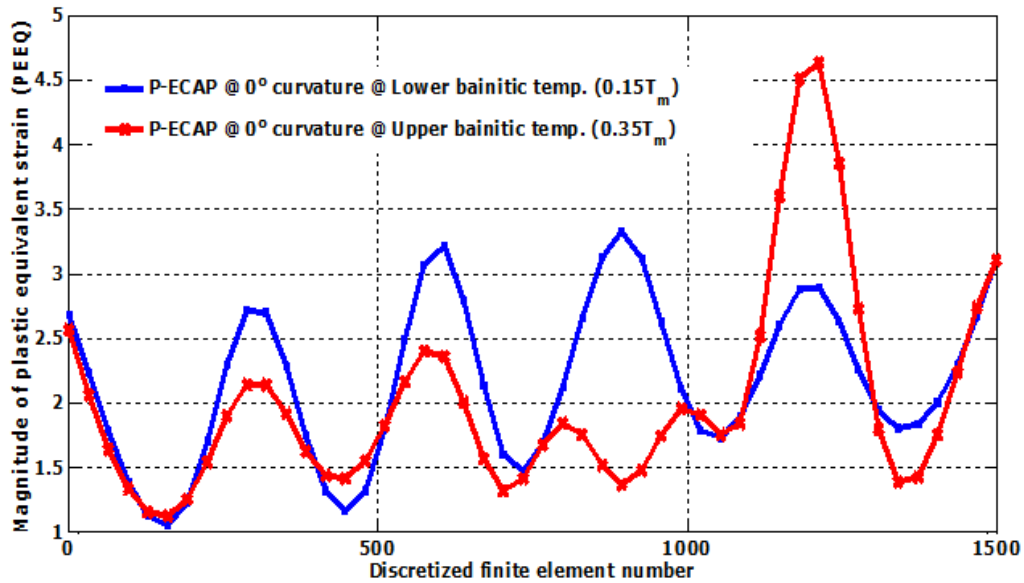
Figure 3: The level of strain inducement on discretized finite elements at the lower and upper bainitic temperatures on P-ECAPed specimen

The result of the overall comparison and analysis of the PEEQ achieved in the specimen at varied deformation temperatures is presented in Fig. (4). This figure shows total compliances to Fig. (5) which portrays that the higher the deformation temperature the lower the overall PEEQ in metals. Consistent sinusoidal trend of temperature activities is seen in the modified ECAP at 0° and 20° curvature except at between discretized element 1100 and 1400 in which there is sudden increase in PEEQ values of modified ECAP at 0° curvature for $0.35T_m$ and $0.5T_m$ temperature (Fig. 6). This could be attributed to the grain growth at elevated temperature.
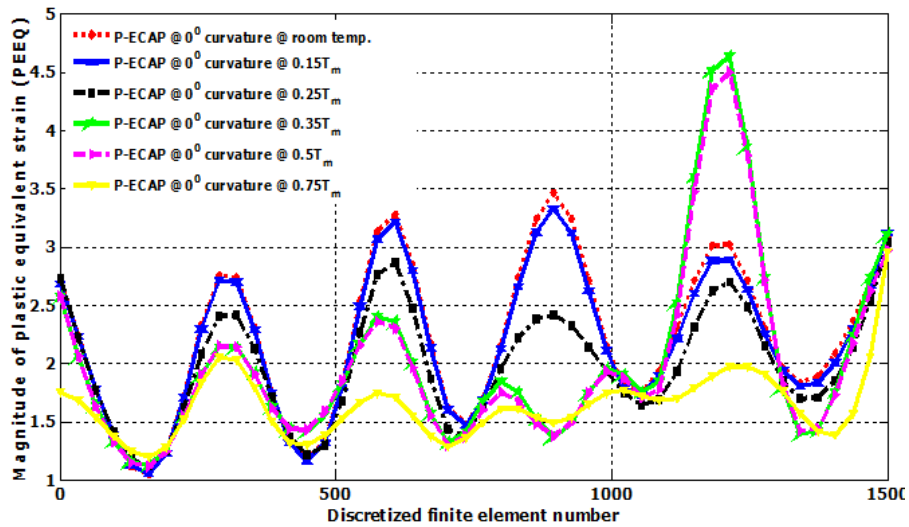
Figure 4: **The level of strain inducement across discretized finite elements at varied temperatures on P-ECAP at 0° curvature**

Figure 4 contains a comparison of PEEQ inducement achieved through both pre-deformation, and modified ECAP at curvature angle 0°. The trend of activities shows that the PEEQ inducement decreases in pre-deformed specimen from the first element up to about element (250) before it tends to increase and eventually a bit and consolidates at element (750). Thereafter, it upshot and came down to form a sinusoidal up at element (1350). On the other hand, modified ECAP at curvature angle 0° have a similar trend from origin up to element (100) before it started increasing and decreasing in magnitude of PEEQ inducement, thereby forming a sinusoidal trend up to element (1100), and then began to decrease. The trend of both activities shows that a likely combination of both technologies can emerge between the different processes. The interwoven nature is significant and this is observable between element (350) and element (1400). Hence, a combination of pre-deformation and ECAP processes is viable for tailoring strain inducement.
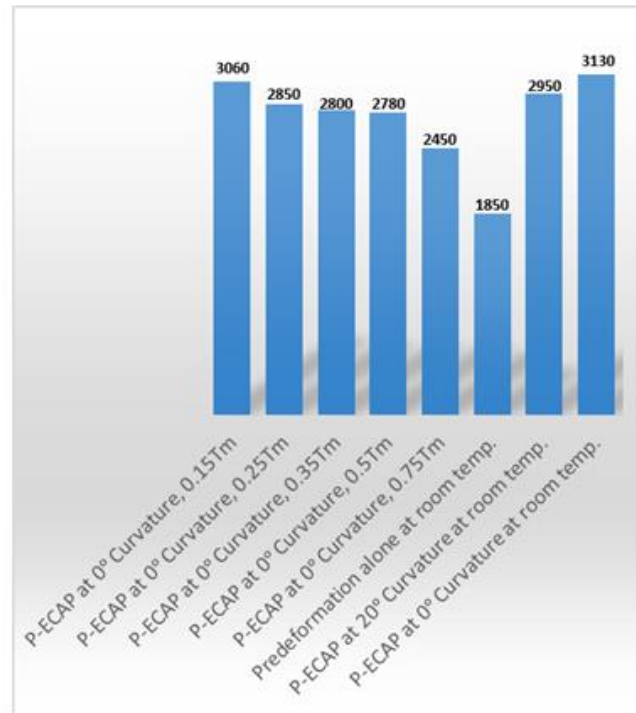
123

Figure 5:   Maximum PEEQ obtained in various strain inducement techniques at varied temperatures

ECAP without pre-deformation has the least overall PEEQ inducement (Fig. 6). This is obvious throughout the activity trend, at the discretized simulation element (500) when the PEEQ values of both ECAP setups were close. Thus, the modified ECAP setups in discourse are feasible and amenable to obtaining huge inducement of plastic strains in metals, as can be seen in Fig. (5).Evidently in Fig. (5), the average magnitude of PEEQ inducement achieved is approximately (2632), while the minimum overall magnitude of strain inducement (1820) achieved is obtained only in pre-deformation process. The maximum strain inducement was obtained on the sample processed with the modified ECAP at curvature angle 0° at room temperature with overall strain value of (3,130), followed by the sample processed with modified ECAP at curvature angle 20° at room temperature with overall strain record of (2,950). On the other hand, the PEEQ inducement recorded at varied temperatures, of $0.15T_m$, $0.25T_m$, $0.35T_m$, $0.5T_m$, to $0.75T_m$, have the strain values as (3,060), (2,850), (2,800), (2,780), and (2,450), respectively. The results indicate that the lower the degree of hotness of the specimen, the higher the amount of grains imposed in the material, and this agrees with the report of (Hanamura et al., 2004 and Beygelzimer et al., 2004).

This assertion could be attributed to the fact that strain relaxation occurs in metals at high temperature levels, hence, cold deformation condition is most appropriate in achieving maximum strain inducement, with resultant grain refinement in metals.
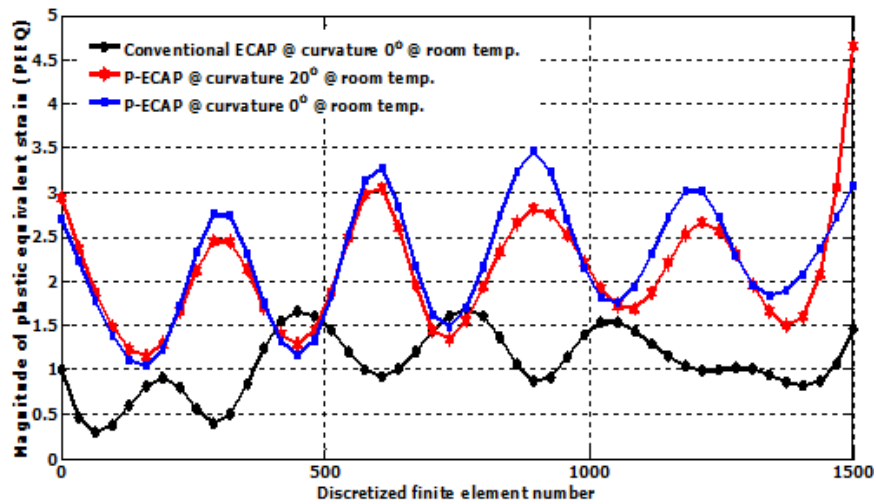

Figure 6: **Strain inducement across discretized finite element specimen subjected to conventional ECAP and P-ECAP (at 0° and 20° curvature), all at room temperature**
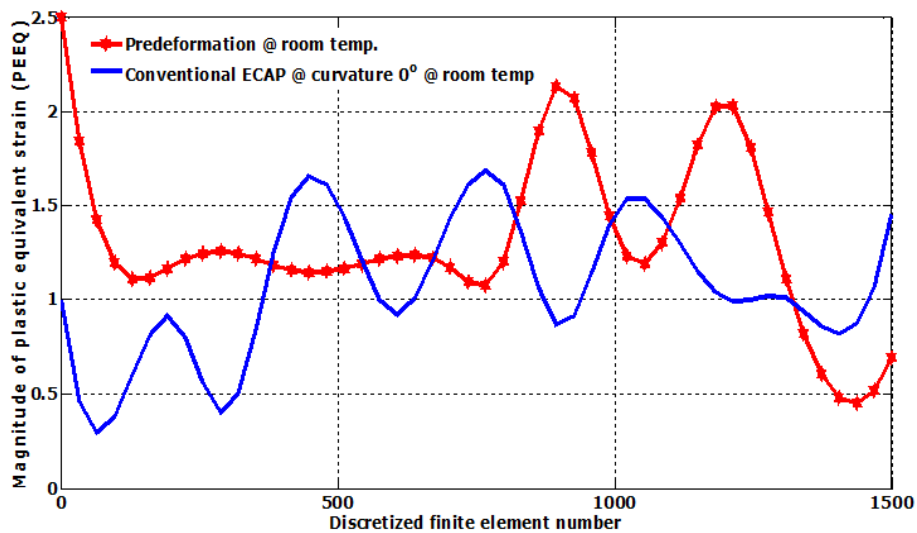

Figure 7: **Comparison of strain inducement achieved at room temperature through pre-deformation alone, and conventional ECAP (at 90° die and 0° curvature)**

At room temperature, Figs. (8 and 11) juxtapose the prevailing respective activities of simulation and numerical PEEQ data, realized through the modified ECAP (at constant die angle 90° and curvature angles: 20° and 0°).

The modified ECAP at curvature angle 0°, has a higher sinusoidal trend. The difference in PEEQ inducement between modified ECAP setups is approximately 6%, which indicates that both the modified ECAP at curvature angle 0° and 20° are capable of achieving reasonable high PEEQ inducement. In a nutshell, the higher PEEQ inducement of the modified ECAP at curvature angle 0°, the higher is the load requirement. This is as a result of the 0° barrier that needed to be overcome for the material to be deformed via the die cavity. Conversely, at 20° curvature, the load requirement is lesser (6 %). These modified and viable ECAP techniques required models that would numerically validate the authenticity of its activities.
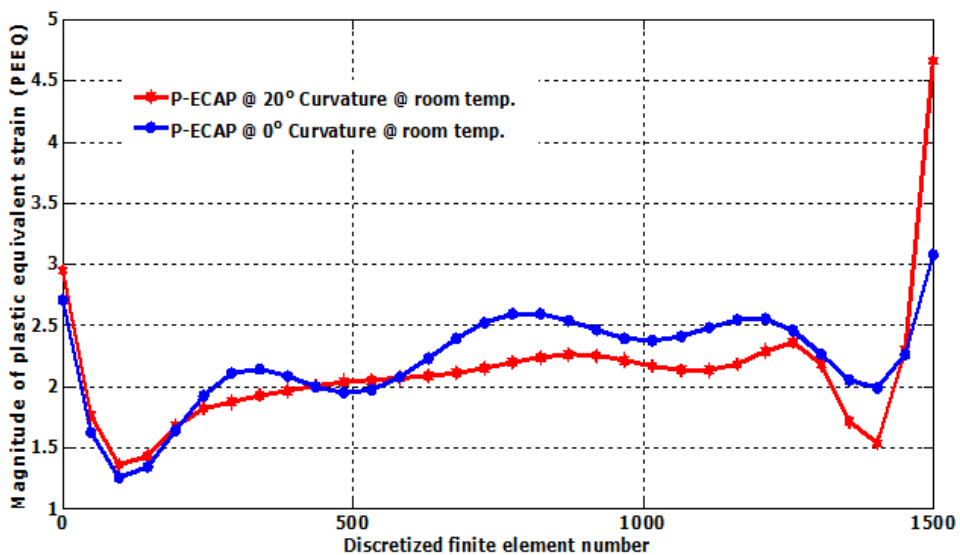

Figure 8: Comparison of strain inducement achieved through P-ECAP at 20° and 0° curvature, both at room temperature
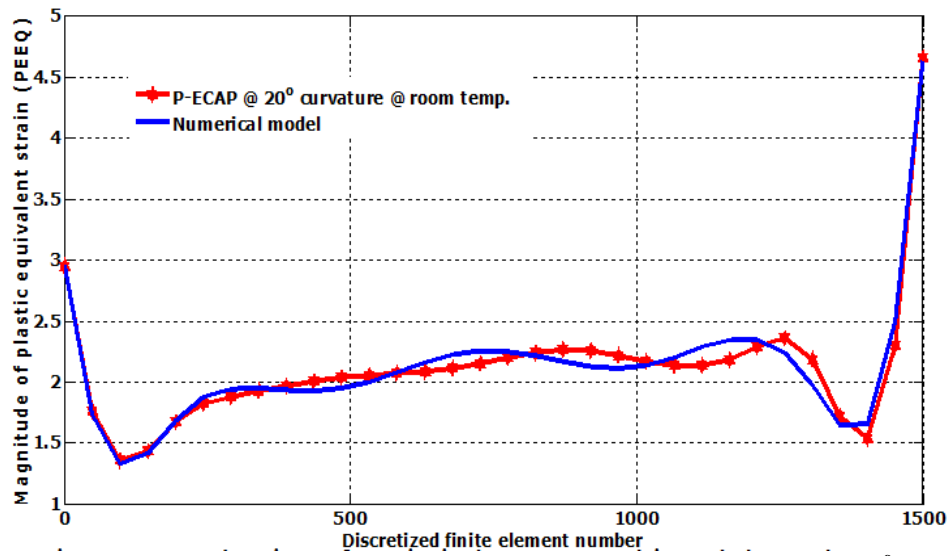
Figure 9: **Evaluation of strain inducement achieved through P-ECAP at 20° at room temperature with its numerical model**
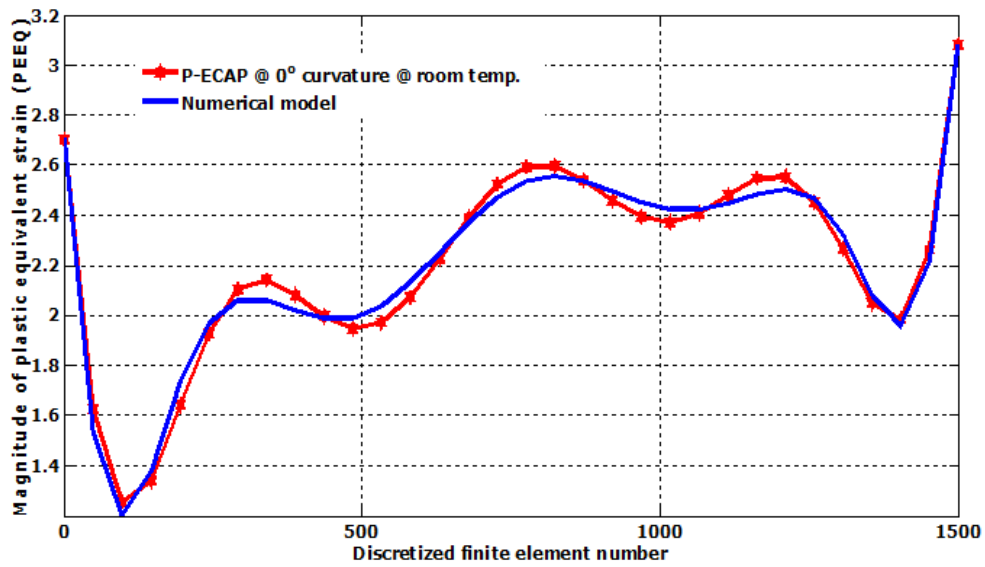

Figure 10: Evaluation of strain inducement achieved through P-ECAP at 0° at room temperature with its numerical model
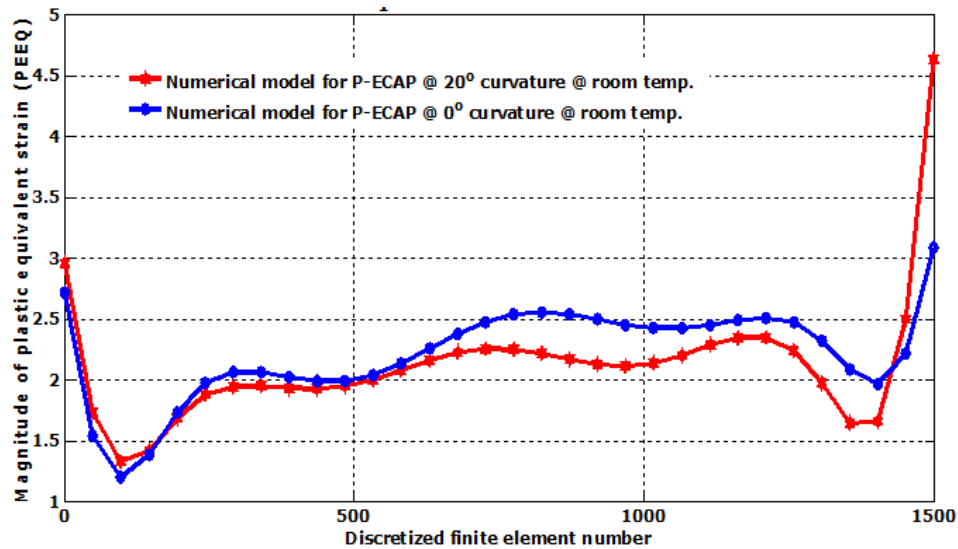
Figure 11: **Evaluation of numerical models for strain inducement achieved through P-ECAP at 20° and 0° curvature at room temperature**

NUMERICAL MODEL

The polynomial regression of the model was evaluated by statistically computing both the coefficient of determination, or R-Square (written as R^2) Eq. (1) and the refinement statistic, adjusted R^2 which does not include any penalty for the number of terms in a model. The R^2 statistics value ranges from 0-1 and it measures the usefulness of the model. The model is a poor predictor if the value of R^2 is closer to zero, but excellent as it approaches 1, (Tofallis, 2015 and MathWorks, 2013).

$$R^2 = \left(\sum (\hat{y}_i - \bar{y})^2 / \sum (y_i - \bar{y})^2 \right) \qquad (1)$$

Where, $y_i, \bar{y}, and\ \hat{y}_i$ are the actual simulation generated data, mean of the actual simulation generated data, and the forecasted or modeled data respectively.

Alternatively,

$$R^2 = 1 - SS_{resid}^2 / SS_{PEEQ} \qquad (1a)$$

While, $adjusted\ R^2 = 1 - \left(R^2 / SS_{PEEQ} \right) * ((n-1)/(n-d-1)) \qquad (2)$

Where, SS_{resid} is the total sum of squares of residuals, $Residuals\ is\ the\ y_{PEEQ} - y_{Model}, SS_{PEEQ}$ is the total sum of squares of

128

dependent variables, n is the number of independent variables, and d is the degree of polynomial. The model equation and the resultant graphs which most suitably and appropriately describe the simulations are generated using high programming tools of MathWork (2013) and are presented in Eqs. (3) and (4).

Pre-deformation and ECAP (with angles: 90° die and 0° curvature) numerical curve equation of best fit of 8th polynomial can be expressed as:

$$y = 0.96073*z^8 + 0.27921*z^7 - 3.7806*z^6 - 0.97421*z^5 + 4.4118*z^4 + 0.92653*z^3 - 1.7267*z^2 - 0.034406*z + 2.2544 \quad (3)$$

Pre-deformation and ECAP (with angles: 90° die and 20° curvature) numerical curve equation at 8th polynomial can be expressed as:

$$y = 0.96073*z^8 + 0.27921*z^7 - 3.7806*z^6 - 0.97421*z^5 + 4.4118*z^4 + 0.92653*z^3 - 1.7267*z^2 - 0.034406*z + 2.2544 \quad (4)$$

where $z = (x - 750.5)/475.78$ for both Eqs. (3) and (4).

The above 8th polynomial Eqs. (3) and (4) were chosen, based on the values of the coefficient of determination, simple R^2 which are above 98% for both grain inducement techniques and its refinement, adjusted R^2 that confirms the adequacy of the model as contained in Table (3), and Figs. (8) and (9). The high level of curve fitting in existence between the raw simulation curve and forecast numerical model curve were demonstrated in Figs. (9) and (10) for the modified ECAP setups.

Table 3: Different R^2 and Adjusted R^2 values from Various Polynomial Equations for two ECAP Processing Angles

ECAP Angles	Degree of Polynomial (th)	SS$_{residuals}$	SS$_{total}$	Simple R^2	Adjusted R^2
	6	0.7085	2.3359	0.7851	0.6419
90° die and 0°	7	0.6804	2.3760	0.8052	0.6347
curvature	8	0.1891	2.8114	0.9873	0.9728
	9	0.1843	2.8122	0.9879	0.9698
	6	0.8943	7.4308	0.8924	0.8206
90° die and 20°	7	0.8413	7.5219	0.9059	0.8236
curvature	8	0.3587	8.1077	0.9841	0.9660
	9	0.2406	8.1742	0.9929	0.9823

To evaluate the degree of accuracy of the models developed as captured in Figs. (9, 10 and 11), the statistical Mean Absolute Deviation Percent (MADP) (Math Works, 2013 and www.vanguardsw.com/business-forecasting). [48 and 49] was used. The MADP is represented in equation (5)

$$\delta_i = \frac{\sum_{i=1}^{n}|N_i - S_i|}{\sum_{i=1}^{n}|S_i|} \quad (5)$$

Where S_i is the actual simulation value of the strain being forecast, N_i is the forecasted numerical model values, and n is the number of different Finite Simulation Discretized Element Numbers considered. The total percentage deviation, (δ) of all the strain induced in the sample is given as:

$$\delta = \sum_{i=1}^{n} \delta_i \quad (6)$$

Furthermore, the arithmetic mean $(\bar{\delta})$ of the total percentage deviation is obtained using:

$$\bar{\delta} = \frac{\sum_{i=1}^{n} \delta_i}{n} \quad (7)$$

From the analysis, the accuracy of the model is obtained by:

$$Accuracy = \left(100 - \bar{\delta}\%\right) \quad (8)$$

Table 4: The Statistical Mean Absolute Deviation Percent of the pre-deformation and ECAP (with 90° die and different angles of curvature)

ECAP Angles	Statistical Mean Absolute Deviation Percent (MADP)			Statistical R-Square	
	$\delta = \sum_{i=1}^{n} \delta_i$	$\bar{\delta} = \frac{\sum_{i=1}^{n} \delta_i}{n}$	Accuracy range (100 - $\bar{\delta}$) (%)	Simple R^2(%)	Adjusted R^2(%)
90° die and 20° curvature	56.39372	3.524608	96.47539	98.41	96.60
90° die and 0° curvature	32.65851	2.041157	97.95884	98.73	97.28

From Tables (3 and 4) it could be deduced that the models for the modified ECAP setups (with die 90°, and curvatures 0° and 20°) have high confidence level, more than 96%. Hence, the degree of accuracy of the model is more than 96 %. Notwithstanding, the experimental investigation and evaluations to validate the

assertions made in this study is underway, and the results will be uncovered in subsequent publication.

Figures (12-20) contain the simulations contour which describes the orientation and distribution of the plastic equivalent strains (PEEQ) induced in the specimen. In all, it obvious that the PEEQ distribution starts from outer surface and cascades toward the center of the specimen, where the PEEQ from both sides will eventually meet. Furthermore, the modified ECAP uses mechanical forces to induce PEEQ on the specimen, as the specimen's surface that had contact with the ECAP die angle 90° experiences mechanical compressive force from surface of the specimen toward the center. The specimen's surface on the other hand, that had contact with the ECAP die angle 0° or 20° experiences mechanical tensile force, also from surface of the specimen toward the center.
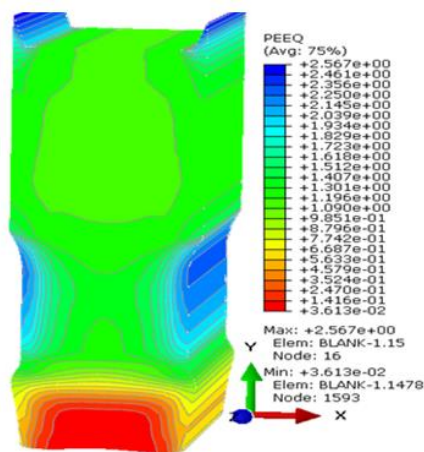
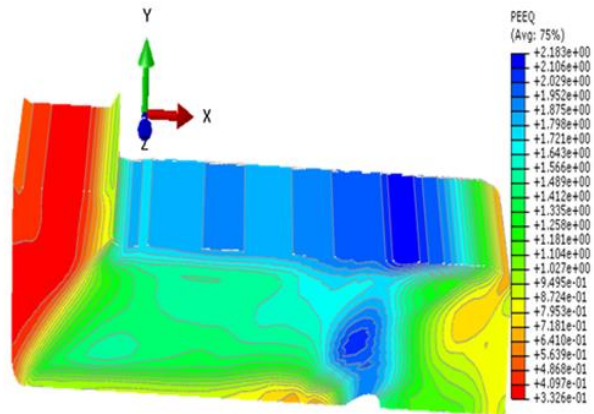**Figure 12: Simulation strain contour for pre-deformation without ECAP at room temperature**

Figure 13: Simulation strain contour for ECAP without pre-deformation at room temperature
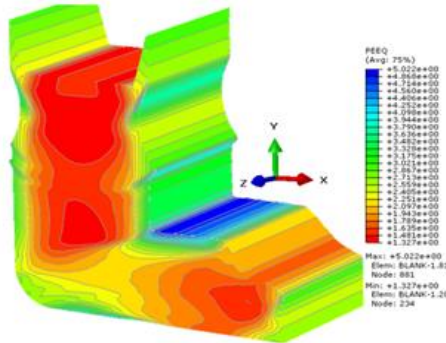
Figure 14: Simulation strain contour for P-ECAP at 20° curvature at room temperature
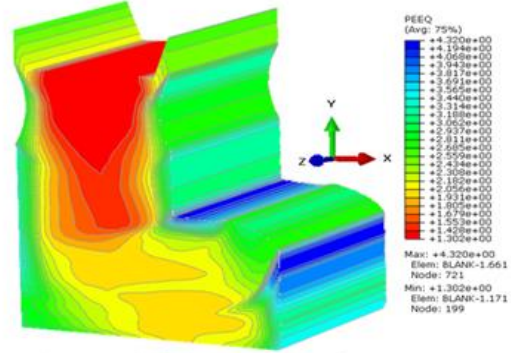

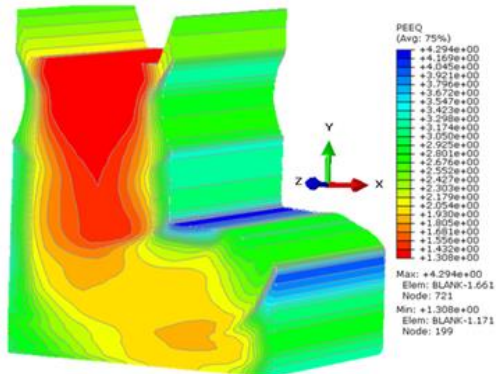**Figure 15: Simulation strain contour for P-ECAP at 0° curvature at room temperature**

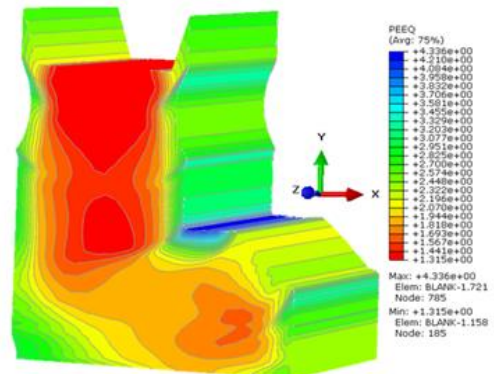**Figure 16: Simulation strain contour for P-ECAP at 0° curvature at $0.15T_m$**

Figure 17: Simulation strain contour for P-ECAP at 0° curvature at $0.25T_m$
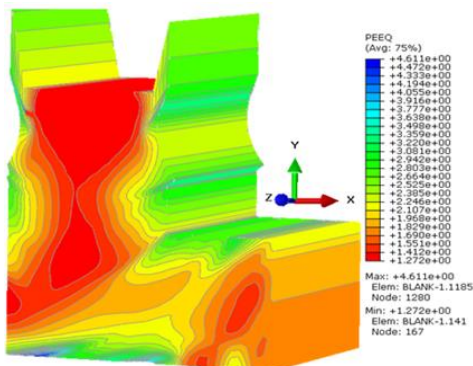

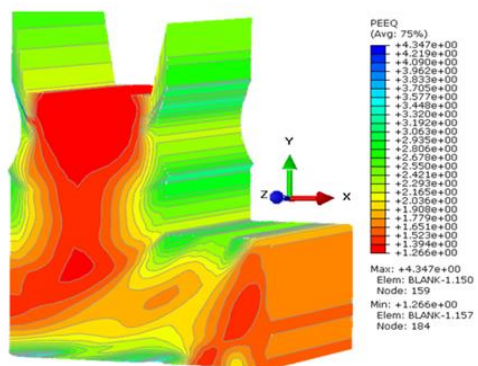**Figure 18: Simulation strain contour for P-ECAP at 0° curvature at $0.35T_m$**

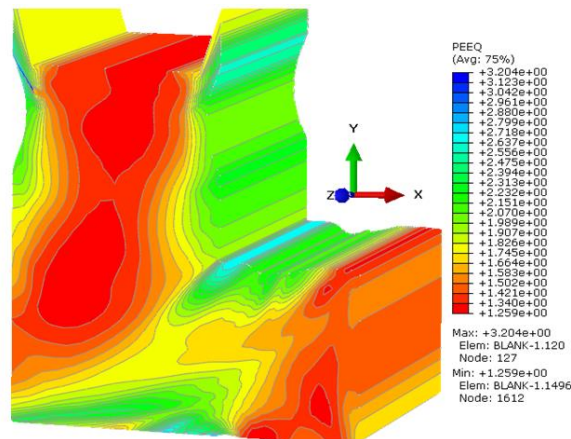**Figure 19: Simulation strain contour for P-ECAP at 0° curvature at $0.5T_m$**

132

Figure 20: Simulation strain contour for P-ECAP at 0° curvature at $0.75T_m$

CONCLUSION

It can be concluded that:

- Ultra-fine grain could be induced in the mild steel through ECAP and P-ECAP techniques
- Numerical analysis reveal that the grains induced in steel through P-ECAP is far higher in magnitude than through the conventional ECAP techniques
- The degree of strain inducement in steel is dependent on the processing parameters
- There is therefore, the possibility to obtain high performance metals at very low temperatures via P-ECAP.

REFERENCES

Alexander D. J. (2007). New Methods for Severe Plastic Deformation Processing. *JMEPEG16*, 360–374. DOI: 10.1007/s11665-007-9054-y.

Alexandrov, I. and Valiev, R. (2001) Developing of SPD Processing and Enhanced Properties in Bulk Nanostructured Metals. *Scripta Materialia*, *44*, 1605-1608. Retrieved from: http://dx.doi.org/10.1016/S1359-6462(01)00783-7

Azushima A, Kopp R, Korhonen A. (2008). Severe plastic deformation (SPD) processes for metals. *CIRP Annals – Manufacturing Technology*. *57*, 716–735.

Beygelzimer Y, Varyukhin V, Orlov D, Synkov S, Spuskanyuk A, Pashinska Y. Zehetbauer M. J., Valiev R. Z. editors. (2004). Nanomaterials by severe plastic deformation. Weinheim, Germany: *Wiley–VCH Verlag*; p. 511.

Bridgman, P.W. (1952). Studies in Large Plastic Flow and Fracture. 1st ed., *McGraw-Hill Book Company*, New York, NY, p. 279.

Chengpeng Wang, Fuguo Li, Qinghua Li, Jiang Li, Lei Wang, Junzhe Dong (2013) A novel severe plastic deformation method for fabricating ultrafine grained pure copper. *Materials and Design 43*, 492–498.

Grange, R. (1966) Strengthening by Austenite Grain Refinement. *Transaction of the American Society Metals*, *1*, 26-29.

Halfa, H. (2014). Recent Trends in Producing Ultrafine Grained Steels. *Journal of Minerals and Materials Characterization and Engineering*, *2*, 428-469. Retrieved from: http://dx.doi.org/10.4236/jmmce. 25047.

Hanamura, T., Yin, F.X. and Nagai, K. (2004) Ductile-Brittle Transition Temperature of Ultrafine Ferrite/Cementite Microstructure in a Low Carbon Steel Controlled by Effective Grain Size. *Iron and Steel Institute of Japan* (*ISIJ*) *International*, *44*: 610-617. Retrieved from: http://dx.doi.org/10.2355/isijinternational.44.610.

Iwahashi Y, Horita Z, Nemoto M, Langdon T. G. (1997) *Acta Mater*; *45*, 4733.

Iwahashi Y., Horita Z., Nemoto M. and Langdon T. G. (1998). The process of grain refinement in Equal-Channel Angular Pressing. *Acta. Mater. 46*(9), 3317-3331. PII: S1359-6454(97) 00494-1.

Kommel, L., Hussainova, I., & Volobueva, O. (2007). Microstructure and properties development of copper during severe plastic deformation. *Materials and Design 28*, 2121–2128.

Korczynsky, M. (1988) Microalloying and Thermo-Mechanical Treatment. In: DeArdo, A.J., Ed., *Proceedings of International Symposium Processing, Microstructure and Properties of HSLA Steels*, Pittsburgh, *1*(3), 169-201.

Krishnaiah, A; Kumaran, K; Chakkingal, U. and Venugopal, P. (2004). finite element analysis of equal channel angular extrusion (ECAE) process. *International Symposium of Research Students on Material Science and Engineering(ISRS)*.

Langdon T. G. (2011). Processing by severe plastic deformation: Historical developments and current impact. *Materials Science Forum*; *667*(669), 9–14. Retrieved from: http://dx.doi.org/10.4028/www.scientific. net/MSF.667-669.9.

Mishra A., Richard V., Gr´egori F., Asaro R. J., Meyers M. A. (2005) Microstructural evolution in copper processed by severe plastic deformation, *Materials Science and Engineering A 410*(411), 290–298.

Mishra R. S, Ma Z. Y. (2005). *Mater Sci Eng*; *R50*, 1.

Najafi-Zadeh, A., Jonas, J. and Yue, S. (1992) Grain Refinement by Dynamic Recrystallization during the Simulated Warm-Rolling of Interstitial Free

Steels. *Metallurgical and Materials Transactions A, 23*, 2607-2617. Retrieved from: http://dx.doi.org/10.1007/BF02658064.

Niikura, N., Fujioka, M., Adachi, A., Matsukura, A., Yokota, T. and Shirota, Y. (2001) New Concepts for Ultra refinement of Grain Size in Super Metal Project. *JMPT*, *117*, 141-146.

Pickering, F. (1990) Some Beneficial Effects of Nitrogen in Steel. In: Korchynsky, M., Gorczyca, S. and Blicharski, M., Eds., *Proceedings of International Symposium Microalloyed Vanadium Steels*, Cracow, *24*(26), 33-62.

Retrieved from: http://www.vanguardsw.com/business-forecasting-101/mean-absolute-deviation-percent-madp/

Rhodes C. G., Mahoney M. W., Bingel W. H., Spurling R., A., Bampton C. C. (1997). *Scripta Mater36*, 69.

Richert M, Liu Q, Hansen N. (1999). *Mater Sci Eng*; *A260*, 275.

Sanusi K. O., and Oliver G. J. (2009). Effects of grain size on mechanical properties of nanostructured copper alloy by severe plastic deformation (SPD) *process. J Eng Design Technol*. *7*(3), 335–341. Retrieved from: http://dx.doi.org/10.1108/17260530910998721.

Saunders and Nutting, J. (1984). Deformation of Metals to High Strains Using Combination of Torsion and Compression, *Metal Sci.*, *18*, 571.

Segal V. M., Dobatkin S. V., Valiev R. Z., Editors. (2004). Equal-channel angular pressing of metallic materials: Achievements and trends. Thematic issue, Part 1, *Russian Metall*, (1), 1–102 [translated from *Metally2004*(1), 3–119.

Segal V. M., Reznikov V. I., Drobyshevskiy A. E. and Kopylov V. I., (1981). *ScriptaMetally, 1*, 115 (English translation: Russian Metallurgy, 1, 99.

Sellars, C. and Whiteman, J. (1979) Recrystallization and Grain Growth in Hot Rolling. *Metal Science*, *13*, 187-194. Retrieved from: http://dx.doi.org/10.1179/msc.1979.13.3-4.187.

Stolyarov, V., Zhu, Y., Lowe, T., Islamgaliev, R. and Valiev, R. (1999) A Two Step SPD Processing of Ultrafine-Grained Titanium. *Nanostructred Materials*, *11*, 947-954. Retrieved from: http://dx.doi.org/10.1016/S0965-9773(99)00384-0.

The MathWorks Inc. (2013). R2013b MATLAB® & Simulink® User Guide.

The SIMULIA (2013). Abaqus/CAE 6.13-1 User's Manual.

Tofallis (2015). A Better Measure of Relative Prediction Accuracy for Model Selection and Model Estimation. *Journal of the Operational Research Society*, *66*(8), 1352-1362.

Toshiro, T., Norio, I. Kaori, M., Suguhiro, F., Mitsuru, Y., Masayuki, W., Manabu, E., Tamotsu, S., Youichi, H. and Yasutaka, O. (2008) Grain Refinement of C-Mn Steel to 1 μm by Rapid Cooling and Short Interval Multi-Pass Hot Rolling in Stable Austenite Region. *Iron and Steel Institute of Japan* (*ISIJ*) *International*, *48*, 1148-1157.

Ueji, R., Tsuji, N., Minamino, Y. and Koizumi, Y. (2002) Ultra-Grain Refinement of Plain Low Carbon Steel by Cold-Rolling and Annealing of Martensite. *Acta Materialia*, *50*, 4177-4189. Retrieved from: http://dx.doi.org/10.1016/S1359-6454(02)00260-4.

Valiev R. Z., Krasilnikov N. A., Tsenev N. K., (1991). *Mater Sci Eng*; *A137*, 35.

Valiev, R. Z., (2003). Paradoxes of severe plastic deformation. *Adv Eng Mater*. *5*(5), 296–300. Retrieved from: http://dx.doi.org/10.1002/adem.200310089.

Valiev, R., Sergueeva, A. and Mukherjee, A. (2003) The Effect of Annealing on Tensile Deformation Behavior of Nanostructure SPD Titanium. *Scripta Materialia*, *49*, 669-674. Retrieved from: http://dx.doi.org/10.1016/S1359-6462(03)00395-6.

Varyutkhin V. N, Beygelzimer Y, Y, Synkov S, Orlov D. (2006). *Mater Sci Forum*; *503*(504), 335.

Wada, T. and Eldis, G. (1982) Transformation Characteristic of 2.25Cr-1Mo Steel, Application of 2.25Cr-1Mo Steel for Thick-Wall Pressure Vessels. ASTM STP 755, *American Society for Testing Materials*, Philadelphia, 343-362.

Yamashita A., Yamaguchi D., Horita Z. & Langdon T. G. (2000). Influence of Pressing Temperature on Microstructural Development in Equal-Channel Angular Pressing. *Mater. Sci. Eng*. *A287*, 100-6.

Zhao, M., Li, J., Zeng, T., Hunag, X., Zhao, Y. and Atrens, A. (2011). The Ductile to Brittle Transition for C-Mn Steel with an Ultrafine Grain Ferrite/Cementite Microstructure. *Materials Science and Engineering A*, *528*, 7228-7237. Retrieved from: http://dx.doi.org/10.1016/j.msea.2011.06.005.